

NJC

Accepted Manuscript



This is an *Accepted Manuscript*, which has been through the Royal Society of Chemistry peer review process and has been accepted for publication.

Accepted Manuscripts are published online shortly after acceptance, before technical editing, formatting and proof reading. Using this free service, authors can make their results available to the community, in citable form, before we publish the edited article. We will replace this *Accepted Manuscript* with the edited and formatted *Advance Article* as soon as it is available.

You can find more information about *Accepted Manuscripts* in the [Information for Authors](#).

Please note that technical editing may introduce minor changes to the text and/or graphics, which may alter content. The journal's standard [Terms & Conditions](#) and the [Ethical guidelines](#) still apply. In no event shall the Royal Society of Chemistry be held responsible for any errors or omissions in this *Accepted Manuscript* or any consequences arising from the use of any information it contains.

ARTICLE

Anti-leishmanial activity of Ni(II), Pd(II) and Pt(II) β -oxodithioester complexes

Cite this: DOI: 10.1039/x0xx00000x

Received 00th January 2012,
Accepted 00th January 2012

DOI: 10.1039/x0xx00000x

www.rsc.org/

Manoj Kumar Yadav^a, Gunjan Rajput^a, Khushboo Srivastava^b, Rakesh Kumar Singh^b, Rajnikant Mishra^c, Michael G. B. Drew^d and Nanhai Singh^{a*}

New functionalized planar β -oxodithioester cis-chelate complexes, $[M(L)_2]$ ($L = L1$, methyl-3-hydroxy-3-(p-bromophenyl)-2-propenedithioate, $M = Ni$ **1**, Pd **5**, Pt **9**; $L2$, methyl-3-hydroxy-3-(p-fluorophenyl)-2-propenedithioate, Ni **2**, Pd **6**, Pt **10**; $L3$, methyl-3-hydroxy-3-(naphthyl)-2-propenedithioate, Ni **3**, Pd **7**, Pt **11**; methyl-3-hydroxy-3-(p-methoxyphenyl)-2-propenedithioate, Ni **4**, Pd **8**, Pt **12**) have been synthesized and characterized by elemental analysis, IR, UV-Vis., 1H and ^{13}C NMR spectroscopy; the structures of **2-4**, **8** and **11** have been elucidated by X-ray crystallography. In all crystal structures the metal has four-coordinate slightly distorted square planar geometry with cis-configuration of the ligands. These complexes have been assessed for their use as anti-leishmanial agents; **7** and **9** showed impressive anti-promastigote and anti-amastigote efficacy with IC_{50} values of $(0.59 \pm 0.10 \mu g/mL, 0.56 \pm 0.10 \mu g/mL)$ and $(IC_{50} 0.85 \pm 0.27, 1.99 \pm 0.08 \mu g/mL)$ respectively. Cytotoxicity assays on both compounds displayed toxicity on the promastigotes but less toxicity against RAW 264.7 cell lines at different concentration. The Pd and Pt complexes exhibit luminescent characteristics in solution originating from the intra ligand charge transfer state.

Introduction

Inorganic complex based drugs are becoming increasingly important because of the co-operative influence of electronic and steric properties of the metal-organic ligand framework that may potentially modify their activity for medicinal applications. The advent of cis-platin, $PtCl_2(NH_3)_2$ the most effective anticancer drug until now, stimulated interest for the design and synthesis of metal complexes for their medicinal applications.¹ Also some Ni(II) and Pd(II) complexes have shown importance in biological systems.²

Leishmaniasis, a parasitic disease has become endemic in developing tropical and subtropical countries. Particularly in the North-East region of Bihar state, India, it has become epidemic due to drug resistance.³ The onset of this disease is caused by the Leishmania genus and transmitted in human by bite of certain infected sand fly. Leishmaniasis is one of the most neglected disease⁴ because of the limited resources available for diagnosis, treatment, and control and its strong association with poverty.⁵ Until now there are no licensed

vaccines against any form of leishmaniasis. Current treatment of the disease is based on chemotherapy, which depends on a few drugs with serious limitations such as high cost, toxicity, difficult route of administration, lack of efficacy in endemic areas and development of resistance.⁶ Apart from the organic compounds, amphotericin B, paromomycin, the orally administered, miltefosine, pentavalent antimonial compound based drugs are in practice.⁷ High toxicity and increasing resistance especially against pentavalent antimonials further complicate this issue in disease endemic regions of the world. The Bi(V) carboxylate, thiocarboxylate⁸ and β -thioxoketone⁹ complexes have been assessed for their antiparasitic activity against *Leishmania major* promastigotes and their cytotoxicity towards human fibroblasts. Recently some Ru(II) clotrimazole (CTZ) complexes have been screened against leishmania.¹⁰ Many heteroleptic Pd, Pt and Ru nitrofurans-thiosemicarbazone complexes have served as potential anti-trypanosomal agents.¹¹ The Pd(II) and Pt(II) mixed-ligand, pyridine-2-thiol N-oxide

and dithiocarbamate complexes have shown anti *T.cruzi* activity.¹²

By comparison, despite synthetic versatility and practical utility,¹³ the β -oxodithioester (O,S-donor) complexes somewhat similar to those with β -thioxoketone ligands have not been explored for their anti-leishmanial activity. It is critical to search for newer metal complex based drugs which will be effective and safe anti-leishmanial agents. The β -oxodithioester ligands (fig.1) used in this work present some interesting features: (i) oxygen is more electronegative than sulphur (ii) sulphur is larger than oxygen and has more diffused p and d orbitals whereas oxygen has no d-orbitals (iii) oxygen is a hard but sulphur is distinctly soft donor (iv) they form highly delocalized six-membered chelate ring about the metal centre (v) the functionalization of substituents on the dithio backbone may influence the electronic and steric properties and (vi) the additional donor atoms on the substituents may induce secondary interactions which are generally not associated with chelating ligands having identical donor atoms. The soft Pd(II) and Pt(II) ions differ from the borderline Ni(II) ion with regard to their preferential bonding with the soft S/hard O donor atoms in accordance of HSAB principle. These features may make significant differences in the stability and M-O/M-S bond polarity and hence the reactivity of the complexes. Furthermore, the metal based drugs are advantageous over organic drugs because of their inherent properties such as variable oxidation states (i.e. redox behaviour), coordination number and geometries and thermodynamic/kinetic characteristics associated with the metals which may induce their Lewis acid activity hence drug activity. Taking into account these facts it was considered worthwhile to undertake the synthesis, crystal structures and anti-leishmanial activity evaluation of new cis-planar chelate β -oxodithioester complexes of Ni(II), Pd(II) and Pt(II). The potential anti-leishmanial activity observed for two complexes are described in this contribution.

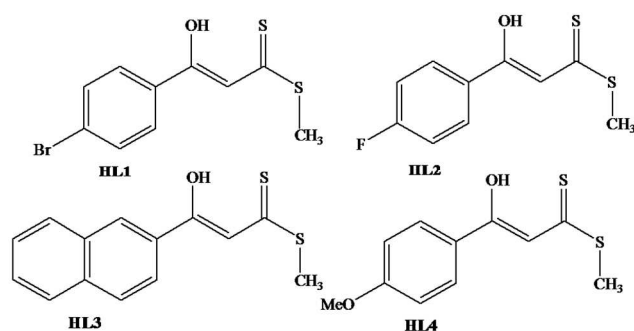


Fig. 1 Structure of ligands used in this work.

Experimental Section

Materials and general methods

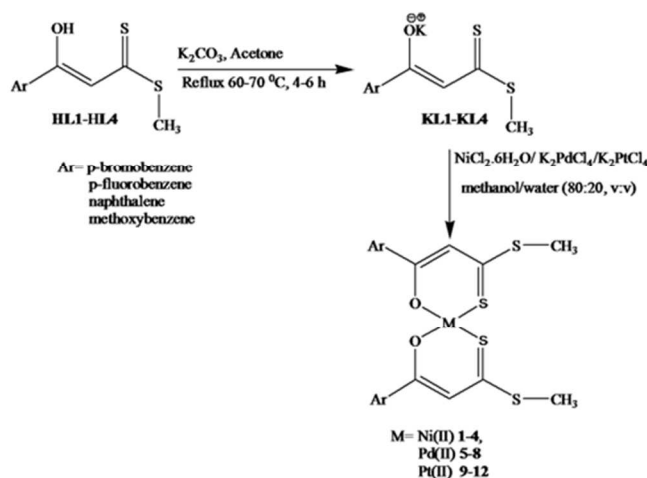
All the experiments were carried out in the open at ambient temperature and pressure unless otherwise quoted. All

chemicals used were reagent grade and obtained from the commercial sources. Solvents were distilled and purified by standard procedures. The ligands methyl-3-hydroxy-3-(p-bromophenyl)-2-propenedithioate (HL1), methyl-3-hydroxy-3-(p-fluorophenyl)-2-propenedithioate (HL2), methyl-3-hydroxy-3-(2-naphthyl)-2-propenedithioate (HL3) and methyl-3-hydroxy-3-(p-methoxyphenyl)-2-propenedithioate (HL4) and their corresponding potassium salts were synthesized as described elsewhere.¹⁴ The experimental details dealing with the elemental analyses (C, H, S), IR, ¹H and ¹³C{¹H} NMR, electronic absorption and luminescent spectra are the same as previously reported.¹⁴

Synthesis of the complexes

[M(L)₂] (M=Ni(II), L = L1 1, L2 2, L3 3, L4 4; Pd(II), L1 5, L2 6, L3 7, L4 8; Pt(II), L1 9, L2 10, L3 11, L4 12)

The homoleptic complexes [M(L)₂] 1-12 were prepared adopting the general procedure as follows (Scheme 1). To a 10 mL stirred methanol-water (80:20, v/v) solution of KL1 (0.28 g, 1 mmol), KL2 (0.31 g, 1 mmol), KL3 (0.27 g, 1 mmol) or KL4 (0.34 g, 1 mmol) was added separately a 10 mL solution of NiCl₂·6H₂O (0.118 g, 0.5 mmol), K₂PdCl₄ (0.163 g, 0.5 mmol) or K₂PtCl₄ (0.207 g, 0.5 mmol) in the same solvent mixture and stirred for 4-8 h. The red-brown Ni(II) and orange coloured Pd(II) and Pt(II) complexes thus obtained as solids were filtered off, washed 3-4 times with methanol followed by diethyl ether. The compounds were purified by recrystallization in dichloromethane; the crystals of 2-4, 8 and 11 were obtained within 3-4 weeks.



Scheme 1 Generalized synthesis of the complexes.

Characterization data

[Ni(L1)₂] 1

Yield: (69 %, 0.219 g). m. p. 275-279°C. Anal. Calcd. for C₂₀H₁₆Br₂NiO₂S₄ (635.70): C 37.82, H 2.54, S 20.20 %. Found: C 37.61, H 2.59, S 19.75 %. IR (KBr, cm⁻¹): ν = 1073 (ν_{C-O}), 1256 (ν_{C-S}), 1586 ($\nu_{C=C}$). ¹H NMR (300.40 MHz, CDCl₃): δ 2.62 (s, 3H, SCH₃), 7.05 (s, 1H, =CH-C(S)-), 7.55 (m, 2H, Ar-H), 7.74-7.68 (m, 2H, Ar-H) ppm. ¹³C{¹H} NMR (75.45 MHz, CDCl₃): δ 23.07 (-SCH₃), 111.08 (=CH-C(S)-), 128.85, 132.68,

143.83, 147.24 (Ar-C), 180.49 (=C-O-), 192.42 (-C=S) ppm. UV-Vis. (CH_2Cl_2 , λ_{max} (nm), ϵ ($\text{M}^{-1}\text{cm}^{-1}$)): 275 (2.67×10^4), 322 (3.28×10^4), 351 (3.26×10^4), 414 (7.9×10^3), 672 (0.6×10^2).

[Ni(L2)₂] 2

Yield: (72 %, 0.185 g). m. p. 279-282°C. Anal. Calcd. for $\text{C}_{20}\text{H}_{16}\text{F}_2\text{NiO}_2\text{S}_4$ (513.29): C 46.80, H 3.14, S 24.99 %. Found: C 46.41, H 3.25, S 24.65 %. IR (KBr, cm^{-1}): $\nu = 1100$ ($\nu_{\text{C-O}}$), 1257 ($\nu_{\text{C=S}}$), 1561 ($\nu_{\text{C=C}}$). ^1H NMR (300.40 MHz, CDCl_3): δ 2.66 (s, 3H, SCH_3), 6.88 (s, 1H, =CH-C(S)-), 6.96 (m, 2H, Ar-H), 7.87-7.82 (m, 2H, Ar-H) ppm. $^{13}\text{C}\{^1\text{H}\}$ NMR (75.45 MHz, CDCl_3): δ 18.7 (- SCH_3), 112.35 (=CH-C(S)-), 115.4, 127.8, 130.5, 145.72 (Ar-C), 183.0 (=C-O-), 209.7 (-C=S-) ppm. UV-Vis. (CH_2Cl_2 , λ_{max} (nm), ϵ ($\text{M}^{-1}\text{cm}^{-1}$)): 256 (4.49×10^4), 285 (3.17×10^4), 326 (6.18×10^4), 368 (7.5×10^4), 413 (2.35×10^4), 668 (1.7×10^2).

[Ni(L3)₂] 3

Yield: (78%, 0.225 g), m. p. 260-264°C. Anal. Calcd. for $\text{C}_{28}\text{H}_{22}\text{O}_2\text{S}_4\text{Ni}$ (577.43): C 58.24, H 3.84, S 22.21 %. Found: C 57.98, H 3.97, S 21.85 %. IR (KBr, cm^{-1}): $\nu = 1118$ ($\nu_{\text{C-O}}$), 1248 ($\nu_{\text{C=S}}$), 1578 ($\nu_{\text{C=C}}$). ^1H NMR (300.40 MHz, CDCl_3): δ 2.66 (s, 3H, SCH_3), 7.24 (s, 1H, =CH-C(S)-), 7.50 (m, 2H, Ar-H), 7.83 (m, 4H, Ar-H), 8.45 (d, 1H, Ar-H) ppm. $^{13}\text{C}\{^1\text{H}\}$ NMR (75.45, CDCl_3): δ 18.3 (- SCH_3), 111.37 (=CH-C(S)-), 122.73-134.96 (Ar-C), 181.2 (=C-O-), 210.8 (-C=S) ppm. UV-Vis. (CH_2Cl_2 , λ_{max} (nm), ϵ ($\text{M}^{-1}\text{cm}^{-1}$)): 264 (8.49×10^4), 301 (4.84×10^4), 324 (6.45×10^4), 359 (6.32×10^4), 416 (1.14×10^4), 663 (1.5×10^2).

[Ni(L4)₂] 4

Yield: (78%, 0.210 g), m. p. 217-220°C. Anal. Calcd. for $\text{C}_{22}\text{H}_{22}\text{NiO}_4\text{S}_4$ (537.36): C 49.17, H 4.13, S 23.87 %. Found: C 48.95, H 4.21, S 23.46 %. IR (KBr, cm^{-1}): $\nu = 1129$ ($\nu_{\text{C-O}}$), 1251 ($\nu_{\text{C=S}}$), 1602 ($\nu_{\text{C=C}}$). ^1H NMR (300.40 MHz, CDCl_3): δ 2.59 (s, 3H, - SCH_3), 3.85 (s, 3H, - OCH_3), 6.88 (s, 1H, =CH-C(S)-), 7.25 (m, 2H, Ar-H), 7.85 (m, 2H, Ar-H) ppm. $^{13}\text{C}\{^1\text{H}\}$ NMR (74.45 MHz, CDCl_3): δ 22.67 (- SCH_3), 55.40 (- OCH_3), 113.99 (=CH-C(S)-), 127.2, 129.14, 133.61, 163.2 (Ar-C), 184.0 (=C-O-), 204.90 (-C=S) ppm. UV-Vis. (CH_2Cl_2 , λ_{max} (nm), ϵ ($\text{M}^{-1}\text{cm}^{-1}$)): 282 (2.81×10^4), 321 (4.81×10^4), 358.5 (5.49×10^4), 410 (1.79×10^4), 668 (1.01×10^2).

[Pd(L1)₂] 5

Yield: (81%, 0.277 g), m. p. 257-261°C. Anal. Calcd. for $\text{C}_{20}\text{H}_{16}\text{Br}_2\text{PdO}_2\text{S}_4$ (682.83): C 35.18, H 2.26, S 18.78 %. Found: C 34.86, H 2.35, S 18.45 %. IR (KBr, cm^{-1}): $\nu = 1094$ ($\nu_{\text{C-O}}$), 1317 ($\nu_{\text{C=S}}$), 1588 ($\nu_{\text{C=C}}$). ^1H NMR (300.40 MHz, CDCl_3): δ 2.66 (s, 3H, - SCH_3), 6.88 (s, 1H, =CH-C(S)-), 6.95-6.97 (m, 2H, Ar-H), 7.86-7.83 (m, 2H, Ar-H) ppm. $^{13}\text{C}\{^1\text{H}\}$ NMR (75.45 MHz, CDCl_3): δ 23.40 (- SCH_3), 110.58 (=CH-C(S)-), 127.64, 133.64, 137.3 142.80 (Ar-C), 175.85 (=C-O-), 190.50 (-C=S) ppm. UV-Vis. (CH_2Cl_2 , λ_{max} (nm), ϵ ($\text{M}^{-1}\text{cm}^{-1}$)): 263 (3.74×10^4), 346 (4.24×10^4), 418 (1.87×10^4).

[Pd(L2)₂] 6

Yield: (81%, 0.227 g), m. p. 247-251°C. Anal. Calcd. for $\text{C}_{20}\text{H}_{16}\text{F}_2\text{PdO}_2\text{S}_4$ (561.02): C 42.82, H 2.87, S 22.86 %. Found: C 42.65, H 2.85, S 22.45 %. IR (KBr, cm^{-1}): $\nu = 1094$ ($\nu_{\text{C-O}}$), 1259 ($\nu_{\text{C=S}}$), 1588 ($\nu_{\text{C=C}}$). ^1H NMR (300.40 MHz, CDCl_3): δ 2.66 (s, 3H, - SCH_3), 6.87 (s, 1H, =CH-C(S)-), 6.96 (m, 2H, Ar-H), 7.86-7.83 (m, 2H, Ar-H) ppm. $^{13}\text{C}\{^1\text{H}\}$ NMR (75.45 MHz,

CDCl_3): δ 21.83 (- SCH_3), 109.60 (=CH-C(S)-), 118.71, 124.32, 136.94, 148.57 (Ar-C), 186.58 (=C-O-), 198.08 (-C=S) ppm. UV-Vis. (CH_2Cl_2 , λ_{max} (nm), ϵ ($\text{M}^{-1}\text{cm}^{-1}$)): 303 (2.28×10^4), 343 (2.62×10^4), 415 (1.65×10^4).

[Pd(L3)₂] 7

Yield: (84%, 0.263 g), m. p. 212-215°C. Anal. Calcd. for $\text{C}_{28}\text{H}_{22}\text{PdO}_2\text{S}_4$ (625.15): C 53.79, H 3.55, S 20.52 %. Found: C 53.68, H 3.66, S 20.35%. IR (KBr, cm^{-1}): $\nu = 1125$ ($\nu_{\text{C-O}}$), 1286 ($\nu_{\text{C=S}}$), 1595 ($\nu_{\text{C=C}}$). ^1H NMR (300.40 MHz, CDCl_3): δ 2.68 (s, 3H, SCH_3), 7.30 (s, 1H, =CH-C(S)-), 7.63 (m, 2H, Ar-H), 8.00 (m, 4H, Ar-H), 8.65 (d, 1H, Ar-H) ppm. $^{13}\text{C}\{^1\text{H}\}$ NMR (75.45, CDCl_3): δ 21.06 (- SCH_3), 113.97 (=CH-C(S)-), 117.05, 121.44, 129.37, 132.83, 134.17, 141.61, 143.95 (Ar-C), 180.91 (=C-O-), 191.95 (-C=S-) ppm. UV-Vis. (CH_2Cl_2 , λ_{max} (nm), ϵ ($\text{M}^{-1}\text{cm}^{-1}$)): 259 (3.50×10^4), 344 (3.06×10^4), 431 (1.41×10^4).

[Pd(L4)₂] 8

Yield: (73%, 0.212g), m. p. 253-256°C. Anal. Calcd. for $\text{C}_{22}\text{H}_{22}\text{PdO}_4\text{S}_4$ (585.09): C 46.16, H 3.79, S 21.92%. Found: C 45.85, H 3.78, S 21.45 %. IR (KBr, cm^{-1}): $\nu = 1124$ ($\nu_{\text{C-O}}$), 1317 ($\nu_{\text{C=S}}$), 1594 ($\nu_{\text{C=C}}$). ^1H NMR (300.40 MHz, CDCl_3): δ 2.59 (s, 3H, - SCH_3), 3.86 (s, 3H, - OCH_3), 6.79 (s, 1H, =CH-C(S)-), 6.93 (m, 2H, Ar-H), 7.91 (m, 2H, Ar-H) ppm. $^{13}\text{C}\{^1\text{H}\}$ NMR (75.45 MHz, CDCl_3): δ 27.81 (- SCH_3), 59.79 (- OCH_3), 114.07 (=CH-C(S)-), 117.62, 122.73, 158.10, 158.91 (Ar-C), 187.87 (=C-O-), 197.61 (-C=S) ppm. UV-Vis. (CH_2Cl_2 , λ_{max} (nm), ϵ ($\text{M}^{-1}\text{cm}^{-1}$)): 346 (3.84×10^4), 413 (2.10×10^4).

[Pt(L1)₂] 9

Yield: (86%, 0.330 g), m. p. 219-223°C. Anal. calcd. for $\text{C}_{28}\text{H}_{22}\text{PtO}_2\text{S}_4$ (713.81): C 31.14, H 2.09, S 17.97 %. Found: C 30.96, H 2.17, S 17.52%. IR (KBr, cm^{-1}): $\nu = 1125$ ($\nu_{\text{C-O}}$), 1287 ($\nu_{\text{C=S}}$), 1595 ($\nu_{\text{C=C}}$). ^1H NMR (300.40 MHz, CDCl_3): δ 2.68 (s, 3H, - SMe), 6.81 (s, 1H, =CH-C(S)-), 7.25-7.87 (m, 2H, Ar-H), 7.87 (m, 2H, Ar-H) ppm. $^{13}\text{C}\{^1\text{H}\}$ NMR (75.45, MHz, CDCl_3): δ 19.3 (- SCH_3), 110.26 (=CH-C(S)-), 126.3, 128.4, 133.7, 140.9 (Ar-C), 179.3 (=C-O-), 209.6 (-C=S) ppm. UV-Vis. (CH_2Cl_2 , λ_{max} (nm), ϵ ($\text{M}^{-1}\text{cm}^{-1}$)): 360 (6.94×10^4).

[Pt(L2)₂] 10

Yield: (81%, 0.263g), m.p. 236-240°C. Anal. Calcd. for $\text{C}_{20}\text{H}_{16}\text{F}_2\text{PtO}_2\text{S}_4$ (649.67): C 36.97, H 2.48, S 19.74%. Found: C 36.75, H 2.45, S 19.42 %. IR (KBr, cm^{-1}): $\nu = 1164$ ($\nu_{\text{C-O}}$), 1224 ($\nu_{\text{C=S}}$), 1595 ($\nu_{\text{C=C}}$). ^1H NMR (300.40 MHz, CDCl_3): δ 2.66 (s, 3H, - SCH_3), 6.90 (s, 1H, =CH-C(S)-), 7.26 (m, 2H, Ar-H), 7.87 (m, 2H, Ar-H) ppm. $^{13}\text{C}\{^1\text{H}\}$ NMR (75.45 MHz, CDCl_3): δ 27.80 (- SCH_3), 109.73 (=CH-C(S)-), 117.62, 129.740, 132.82, 137.61, 144.43, 147.57 (Ar-C), 183.30 (=C-O-), 201.61 (-C=S) ppm. UV-Vis. (CH_2Cl_2 , λ_{max} (nm), ϵ ($\text{M}^{-1}\text{cm}^{-1}$)): 255 (3.16×10^4), 309 (3.1×10^4), 368 (5.25×10^4), 403 (3.95×10^3).

[Pt(L3)₂] 11

Yield: (83%, 0.296 g), m. p. 205-208°C. Anal. Calcd. for $\text{C}_{28}\text{H}_{22}\text{PtO}_2\text{S}_4$ (713.81): C 47.11, H 3.11, S 17.97 %. Found: C 46.85, H 3.15, S 17.62 %. IR (KBr, cm^{-1}): $\nu = 1131$ ($\nu_{\text{C-O}}$), 1302 ($\nu_{\text{C=S}}$), 1594 ($\nu_{\text{C=C}}$). ^1H NMR (300.40 MHz, CDCl_3): δ 2.68-2.64 (s, 3H, SCH_3), 6.85 (d, 1H, =CH-C(S)-), 7.56 (m, 2H, Ar-H), 7.98 (m, 4H, Ar-H), 8.47 (d, 1H, Ar-H) ppm. $^{13}\text{C}\{^1\text{H}\}$ NMR (75.45, CDCl_3): δ 27.82 (- SCH_3), 109.38 (=CH-C(S)-),

126.84, 128.20, 131.04, 135.64, 141.82, 145.26, 146.27 (Ar-C), 184.31 (=C-O-), 200.80 (-C=S) ppm. UV-Vis. (CH_2Cl_2 , λ_{max} (nm), ϵ ($\text{M}^{-1}\text{cm}^{-1}$)): 296 (6.35×10^4), 357 (7.49×10^4).

[Pt(L4)₂] **12**

Yield: (76%, 0.256 g), m. p. 276–280 °C. Anal. Calcd. for $\text{C}_{22}\text{H}_{22}\text{PtO}_4\text{S}_4$ (673.75): C 39.22, H 3.29, S 19.04 %. Found: C 39.07, H 3.37, S 18.64 %. IR (KBr, cm^{-1}): $\nu = 1175(\nu_{\text{C-O}})$, $1253(\nu_{\text{C-S}})$, $1595(\nu_{\text{C=C}})$. ^1H NMR (300.40 MHz, CDCl_3): δ 2.65 (s, 3H, -SCH₃), 3.87 (s, 3H, -OCH₃), 6.95–6.92 (m, 2H, Ar-H), 7.09 (s, 1H, =CH-C(S)-), 8.02 (m, 2H, Ar-H) ppm. ^{13}C { ^1H } NMR (74.45 MHz, CDCl_3): δ 22.69 (-SCH₃), 55.6 (-OCH₃), 112.89 (-CH=C(S)-), 117.62, 122.73, 158.10, 158.97 (Ar-C), 187.87 (=C-O-), 200.50 (-C=S) ppm. UV-Vis. (CH_2Cl_2 , λ_{max} (nm), ϵ ($\text{M}^{-1}\text{cm}^{-1}$)): 344 (4.08×10^4), 424 (1.72×10^4).

X-ray structure determinations

Single crystals of the complexes **2-4**, **8** and **11** were grown by slow evaporation of the CH_2Cl_2 solution of products. The X-ray diffraction data were collected on an Oxford X-calibur CCD diffractometer at 293 K using Mo K α radiation. Data reduction were carried out using the CrysAlis program.¹⁵ The structures were solved by direct methods using SHELXS-97¹⁶ and refined on F^2 by full matrix least squares method using SHELXL-97.¹⁷ Non-hydrogen atoms were refined anisotropically and hydrogen atoms were geometrically fixed with thermal parameters equivalent to 1.2 times that of the atom to which they were bonded. Diagrams for all complexes were prepared using ORTEP¹⁸ and Mercury software.¹⁹

Bioevaluation methods: *In vitro* anti-leishmanial assay

Material and methods

To evaluate anti-leishmanial activity a cloned line of *Leishmania donovani* promastigotes (2012) was used throughout this study, which is maintained in the laboratory. In order to assess the activity of compounds against the amastigote stage of the parasites, mouse macrophage cell lines (J-774A.1) were used. The promastigote forms of parasites were maintained *in vitro* in Dulbecco minimum essential medium (DMEM, Invitrogen, USA) supplemented with 10% FBS (Invitrogen, USA) and antibiotics (gentamycin 20 $\mu\text{g}/\text{mL}$, streptomycin 100 $\mu\text{g}/\text{mL}$, penicillin 100 U/mL, Sigma Chemicals, USA) at pH 7.2 in a BOD incubator at 25°C. For drug assays logarithmic phase parasites were harvested.

Preparation of stock solutions. Stock solutions of test samples were prepared initially in DMSO at 10 mg/mL concentration and further diluted with fresh complete medium and sterilized by filtration.

A: *In vitro* antipromastigote activity

For determination of the anti-leishmanial activity of compounds, promastigotes (1×10^6 cells/100 μL /well) were seeded in a 96-well microtiter plate in the presence of 100 μL of compounds in each well (which were 2 fold serially diluted over seven points starting from 100 $\mu\text{g}/\text{mL}$, so final concentration of compounds in wells which ranges from 50

$\mu\text{g}/\text{mL}$ to 0.78 $\mu\text{g}/\text{mL}$) and were further incubated for 48 h. After 48h, the anti-leishmanial activities were evaluated by a MTT (3-[4,5-methylthiazol-2-yl]-2,5-diphenyltetrazolium bromide) assay, which is based on the reduction of the tetrazolium dye to insoluble formazan by the mitochondrial enzymes (Mosmann, 1983). Briefly, 30 μL (5 mg/mL) of MTT was added to each well, incubated for 2h at 37°C and centrifuged at 3000 rpm for 5 min. The supernatant was removed, the parasites were washed in PBS, and the precipitated formazan was dissolved in DMSO (150 μL). Cell viability was measured by absorbance at 540 nm on an ELISA plate reader. All experiments were repeated three times for each drug in duplicates.

Data analysis

The inhibition of parasitic growth is determined by comparison of the activity of treated parasites with that of untreated controls using the formula, Percentage Inhibition = $N-n/N \times 100$, where N is the average OD of control wells and n is the average OD of treated wells. The cytotoxic effect are expressed as 50% lethal dose, i.e., as the concentration of a sample which provoked a 50% reduction in cell viability compared to cell in culture medium alone. Results were expressed as a concentration resulting in 50% inhibition (IC_{50}) \pm standard deviation that was calculated by linear interpolation (Huber and Koella, 1993) as follows,

$$\log(\text{IC}_{50}) = \log(X1) + (50-Y1)/(Y2-Y1) [\log(X2) - \log(X1)]$$

where X1: Concentration of the drug that gives a % inhibition of the parasitaemia $Y > 50\%$,

X2: Concentration of the drug that gives a % inhibition of the parasitaemia $Y < 50\%$.

These cytotoxicity assay were performed for compounds having antipromastigote activity with $\text{IC}_{50} < 100$.

B. Macrophage-amastigote *in vitro* test model

***In vitro* anti-amastigote activity.** J774.1 cells were seeded in 24 well plate at a density of 4×10^5 cells/100 μL /well in DMEM medium containing 10% FBS and plates were incubated at 37°C in 5% CO_2 incubator. After 24 h, the medium was replaced with fresh medium containing stationary phase promastigotes in 7:1 parasite to cell ratio, and incubated at 37°C in CO_2 incubator for 4–6 h. After incubation, cells were washed 2–3 times to remove non-internalized promastigotes. The test compounds (200 μL) were added two-fold serially diluted with complete DMEM medium over seven concentrations (50 – 0.78 $\mu\text{g}/\text{mL}$) and then incubated for 48 h. After this period the cells were washed with phosphate buffer saline (0.02 M, pH 7.2), methanol fixed and stained with Giemsa to count live amastigotes in macrophage by bright-field microscopy.²⁰ The anti-amastigote activities of compounds were determined microscopically by counting number of amastigotes by examining at least 200 infected macrophages per experiment. IC_{50} values were determined by monitoring the reduction in the mean percentage of infected

macrophages or by the mean reduction in the number of amastigotes per macrophage in drug treated cultures in relation to non treated cultures.²¹ Miltefosine was used as the reference standard drug and as a control.

C: Cytotoxicity assay

The cell toxicity of compounds was evaluated on RAW264.7 cells as described elsewhere.²² Briefly, RAW264.7 macrophage cells were maintained in DMEM medium supplemented with 10 % FBS at 37°C in a humidified mixture of 5% CO₂ atmosphere. Macrophages (1×10^6 cells/mL) were seeded in 96-well microtiter plate in the presence of compounds, which were 2-fold serially diluted over six concentrations (100 to 0.78125 µg/mL) in DMEM medium and further incubated for 48 h. Cells without compounds (untreated cells) were used as control and considered as 100 percent viable cells. The cell viability were assayed using MTT, viability = mean absorbance of treated cells/mean absorbance of non-treated cells x 100. The cytotoxicity assays were performed for compounds having anti-promastigote activity, IC₅₀<100. The IC₅₀ values were calculated using nonlinear regression analysis.

Results and Discussion

Synthesis and characterization

Treatment of a water- methanol solution containing two equivalents of the potassium salt of the ligands, **KL1-KL4** with one equivalent of NiCl₂.6H₂O, K₂PdCl₄ or K₂PtCl₄ in the same solvent mixture yielded air and moisture stable homoleptic complexes **1-12** in good yield (Scheme 1). The complexes have been characterized by elemental analysis, IR, UV-Vis., ¹H and ¹³C NMR and their structures have been elucidated by X-ray crystallography. The luminescent behaviour of the complexes has been studied in CH₂Cl₂ solution. All the complexes were screened for activity against leishmanial parasite; only **7** and **9** have shown potential anti-leishmanial activity.

Spectroscopy

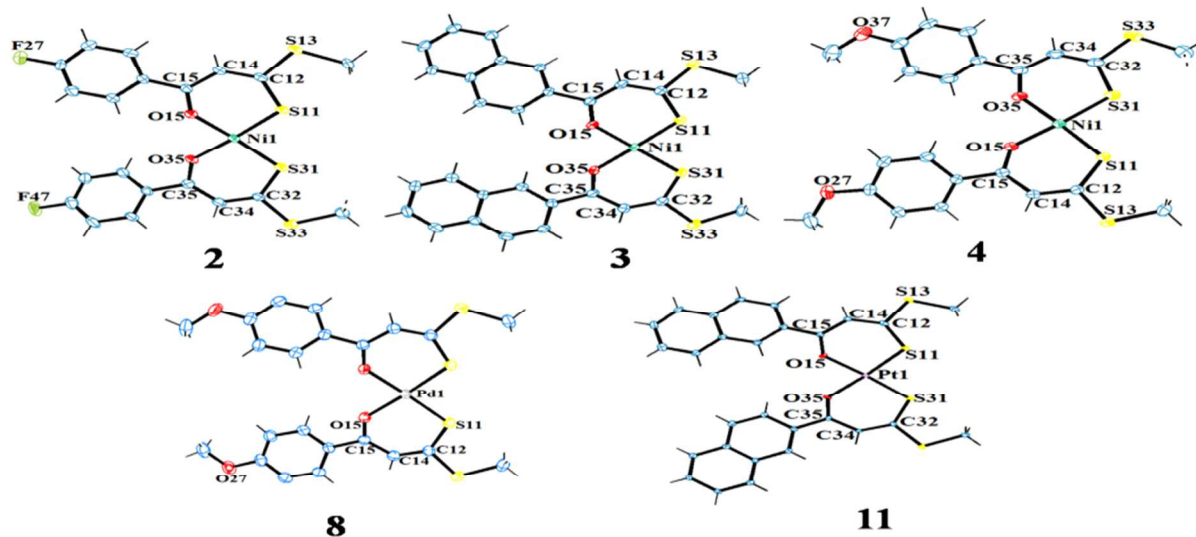
In the IR spectra, complexes **1-12** show bands at 1073-1175, 1224-1285 and 1578-1595 cm⁻¹ for the ν_{C-O}, ν_{C=S} and ν_{C=C} vibrations respectively diagnostic of O,S-coordination of β-oxodithioester ligands.^{14, 23} In the ¹H NMR spectra the ligands **HL1- HL4** (for details see ESI) display a single resonance in the δ 14.89-15.17 ppm range due to -OH proton, which is not observed in the complexes **1-12**. The peak for the vinylic proton is found at δ 6.72-7.10 ppm and δ 6.79-7.24 ppm for the ligands and complexes respectively. In the ¹³C{¹H} spectra the resonances at δ 167.10-169.51 and δ 175.85-187.87 ppm correspond to the C-OH carbon in the free ligands and the

complexes respectively. The vinylic carbon at δ 107.08-108.22 ppm for the ligands is observed at δ 109.38-114.07 ppm in the complexes with a downfield shift of approximately δ 4-6 ppm. The -C=S carbon at δ 215.02-218.0 ppm for the free ligands is significantly upfield shifted at δ 192.42-210.8 ppm in the complexes showing metal-ligand coordination.²³

Crystal Structures

The single crystals of the complexes **2-4**, **8** and **11** were grown in dichloromethane solution. The crystal parameters and selected bond distances and angles are given in table 1 and 2 respectively. Their ORTEP diagrams are as shown in Figure 2. The asymmetric unit of **2-4** and **11** contains one discrete molecule whereas that of **8** contains half a molecule thus in this with the metal atom lying on a twofold axis. All the complexes show a distorted square planar geometry in a *cis* fashion coordinated *via* O15, S11, O35, S31 atoms. The distortion arises due to larger bite angles S11-M1-O15 and S31-M1-O35 at 95.59(6)–96.11(9)° for Ni complexes (**2-4**); 96.26(12) and 96.11(12)° respectively for **11** and S11-M1-O15 angle at 94.72(5)° for **8**. In the five structures, the S₂O₂ equatorial plane shows r.m.s. deviations of 0.036, 0.064, 0.013, 0.000, 0.026 Å with the metal 0.013(1), 0.006(1), 0.011(1), 0.000, 0.007(1) Å from the plane in **2-4**, **8** and **11** respectively. As expected with their size, the M-O distances for Ni complexes, **2-4** are significantly shorter at (1.847(3)–1.860(2) Å) than the Pd complex **8**, at 2.022(1) and the Pt complex, **11** at (2.011(4), 2.022(4) Å). Similarly, the M-S distances of 2.126(1)–2.148(1) Å are shorter in **2-4** than **8** at 2.231(1) Å and **11** at 2.229(1) / 2.243(2) Å. The C12-C14 / C14-C15 distances at 1.352(5) - 1.376(4) / 1.383(6)–1.411(5) Å for **2-4**, 1.372(3) / 1.395(3) Å for **8** and 1.411(8) / 1.397 (8) Å for **11** are intermediate between single and double bond lengths. In all structures the C12-S11 bonds are shorter than the C12-S13 bonds with range of 1.683(4)-1.707(3) Å and 1.742(3)-1.762(3) Å respectively but both fall in the range between carbon-sulphur single and double bond lengths.²⁴

The six-membered chelate ring is approximately planar in all structures with r.m.s deviations in the range 0.012-0.044 Å in the five structures. The two rings intersect at small angles 4.0, 8.9, 0.8 0.0, 4.9° with variations that are no doubt due to packing effects. As is apparent from figure 2, the substituents on the six-membered ring are approximately coplanar so that all molecules are essentially planar. The supramolecular structures of the complexes are sustained *via* weak intermolecular C-H...S, C-H...O and CH...π interactions (table 3, ESI).

Fig-2. Molecular structures of **2-4, 8** and **11** with displacement ellipsoids at 30% probability.**Table 1** Crystal refinement parameters

Compound	2	3	4	8	11
Chemical Formula	C ₂₀ H ₁₆ F ₂ NiO ₂ S ₄	C ₂₈ H ₂₂ NiO ₂ S ₄	C ₂₂ H ₂₂ NiO ₄ S ₄	C ₂₂ H ₂₂ O ₄ PdS ₄	C ₂₈ H ₂₂ O ₂ PtS ₄
Formula Weight	513.28	577.41	537.35	585.04	713.78
Crystal system	triclinic	monoclinic	monoclinic	tetragonal	monoclinic
Space group	P-1	P2 ₁ /c	P2 ₁	I4 ₁ /a	P2 ₁ /c
<i>a</i> (Å)	12.2291(9)	24.946(4)	12.1110(4)	17.4781(5)	13.3438(5)
<i>b</i> (Å)	4.0160(4)	5.8062(10)	7.1701(3)	17.4781(5)	16.6915(7)
<i>c</i> (Å)	23.0003(15)	17.003(3)	13.5948(5)	15.3714(4)	11.6650(5)
α (°)	75.300(7)	90.00	90.00	90.00	90.00
β (°)	84.316(6)	91.800(13)	98.151(3)	90.00	106.870(4)
γ (°)	69.691(8)	90	90	90	90
<i>V</i> (Å ³)	1024.62(14)	2461.5(7)	1168.61(8)	4695.7(2)	2486.31(18)
<i>Z</i>	2	4	2	8	4
ρ_{calc} (g cm ⁻³)	1.664	1.558	1.527	1.655	1.904
<i>T</i> (K)	293(2)	293(2)	293(2)	293(2)	150(2)
μ (Mo <i>K</i> α) (mm ⁻¹)	1.387	1.154	1.214	1.173	6.005
<i>F</i> (000)	524	1192.0	556	2368	1392
Reflections collected	8853	18304	5096	9818	15140
Independent reflns	4468	5584	3660	2626	7087
Reflections with <i>I</i> > 2 σ (<i>I</i>)	2966	3643	3139	1980	5020
Final indices [<i>I</i> > 2 σ (<i>I</i>)] <i>R</i> ₁ ^a , <i>wR</i> ₂ ^b	0.0545, 0.1001	0.0664, 0.1555	0.0343, 0.0729	0.0327, 0.0750	0.0498, 0.0819
<i>R</i> ₁ ^a , <i>wR</i> ₂ ^b [all data]	0.0904, 0.1191	0.1046, 0.1780	0.0450, 0.0781	0.0526, 0.0811	0.0839, 0.0942
GOF	0.993	1.007	0.946	1.076	0.925
CCDC	1055639	1055640	925921	1055641	1055642

$$^a R_1 = \sum |F_o| - |F_c| / \sum |F_o|, \quad ^b R^2 = \{[\sum w(F_o^2 - F_c^2) / \sum w(F_o^2)^2]\}^{1/2}, \quad w = 1/[\sigma^2(F_o^2) + (xP)^2], \quad \text{where } P = (F_o^2 + 2F_c^2)/3$$

Table 2 Selected bond distances and angles for **2-4**, **8** and **11**.

	Bond lengths (Å)				
	2 (M = Ni)	3 (M = Ni)	4 (M = Ni)	8 (M = Pd) ^a	11 (M = Pt)
M-O15	1.847(3)	1.856(3)	1.849(2)	2.0223(2)	2.011(4)
M-O35	1.860(2)	1.853(3)	1.848(2)	-	2.022(4)
M-S11	2.148(1)	2.132(1)	2.137(1)	2.2314(1)	2.230(2)
M-S31	2.146(1)	2.126(1)	2.141(1)	-	2.244(2)
C15-O15	1.269(4)	1.254(5)	1.269(3)	1.266(3)	1.285(7)
C15-C14	1.411(5)	1.383(6)	1.399(4)	1.395(3)	1.411(8)
C12-C14	1.352(5)	1.368(5)	1.376(4)	1.372(3)	1.397(8)
C12-S11	1.705(4)	1.683(4)	1.707(3)	1.697(3)	1.697(7)
C12-S13	1.762(3)	1.749(4)	1.744(3)	1.757(3)	1.742(6)
	Bond Angles (°)				
O15-M-S11	95.68(8)	96.11(9)	95.59(6)	94.72(5)	96.26(12)
O15-M-S31	176.01(8)	175.88(10)	176.79(11)	175.17(6)	175.55(12)
O15-M-O35	81.21(11)	83.29(12)	81.49(9)	82.88(10)	79.58(16)
S11-M-S31	87.19(4)	84.77(4)	87.28(3)	87.97(4)	88.07(6)
S11-M-O35	176.58(9)	176.52(10)	177.08(7)	-	175.46(13)
S31-M-O35	95.99(9)	96.07(9)	95.64(7)	-	96.11(12)

^ain **8** S31 and O35 are S11\$1, O31\$1 where \$1 represents symmetry element -x, 3/2-y,z.

Absorption and emission spectra

The UV-Vis. absorption and photoluminescence spectra of the complexes were recorded in dichloromethane solution at room temperature and displayed in Figure 4 and 5 respectively. The Ni (**1-4**) complexes exhibit bands near 260-415 nm ($\epsilon = 0.79$ - $8.49 \times 10^4 \text{ M}^{-1}\text{cm}^{-1}$); the high energy bands are assigned to intra ligand (ILCT) whereas the low energy bands are assigned to ligand to metal (LMCT) charge transfer transitions. In these complexes a high energy band near 670 nm ($\epsilon = 0.6$ - $1.01 \times 10^2 \text{ M}^{-1}\text{cm}^{-1}$) corresponds

to the d-d transition. The analogous Pd and Pt complexes display absorptions near 250-431 nm ($\epsilon = 1.40$ - $6.94 \times 10^4 \text{ M}^{-1}\text{cm}^{-1}$) assignable to ILCT and metal perturbed ILCT transitions. When excited at 350 nm the Pd (**5-8**) and Pt (**9-12**) complexes show an unstructured emission band near 440 nm originating from the metal perturbed intra ligand charge transfer (ILCT) state. As expected all the Ni complexes are weakly luminescent due to their well known quenching behaviour

because of the occurrence of d-d band in the visible region.²⁵

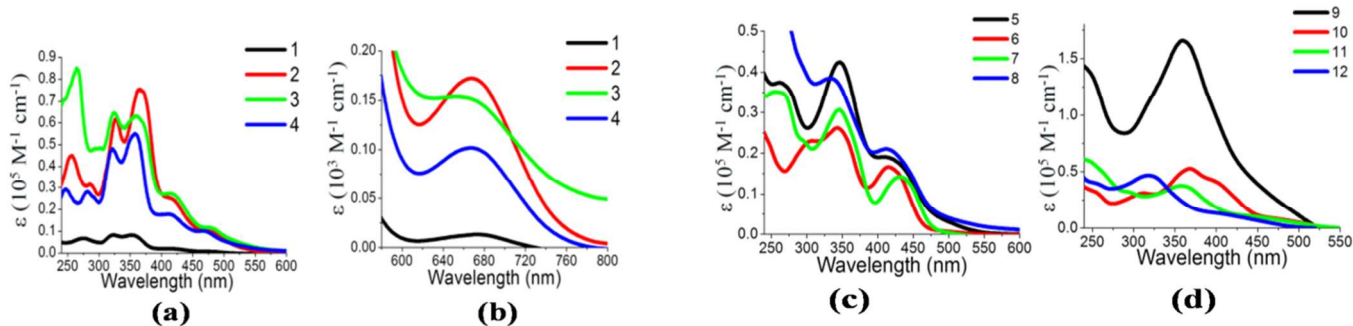


Fig.3 Absorption spectra for (a) Ni (**1-4**) and (b) d-d transitions in **1-4** (c) Pd (**5-8**) (d) Pt (**9-12**) complexes in dichloromethane solution at room temperature.

ARTICLE

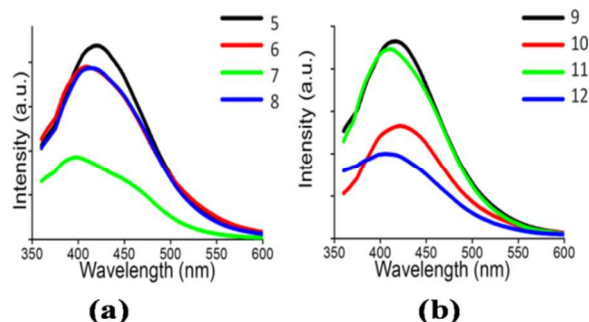


Fig. 4 Photoluminescence spectra of (a) Pd (5-8) and (b) Pt (9-12) complexes in dichloromethane solution at room temperature.

Anti-leishmanial studies

All the metal complexes were evaluated for their antileishmanial activities but out of these only two showed significant *in vitro* antileishmanial promastigote and intracellular amastigote activities than the standard drug Miltefosine. The antiparasitic activities of these metallic

compounds have been demonstrated against *L. donovani* responsible for visceral leishmaniasis.

In this present study Pt (9) and Pd (7) complexes showed good anti-promastigote activity having IC_{50} values 0.59 ± 0.100 $\mu\text{g/mL}$ and 0.56 ± 0.10 $\mu\text{g/mL}$ respectively (Table 3, Fig. 5). Pt and Pd containing compound showed 80% parasitic inhibition at 50 $\mu\text{g/mL}$ and on visual observation it showed loss of flagellum, rounded morphology with substantial reduction in size as compared to control promastigotes, cell shrinkage and cell condensation may be cause of apoptosis, which may be possible cause of cell death, an exerted effect of Pt (9) and Pd (7) complex compounds. Anti-amastigote activity of these compounds has IC_{50} 0.85 ± 0.272 and 1.99 ± 0.08 $\mu\text{g/mL}$ respectively (Table 3, Fig. 5). Cytotoxicity assay on both the compounds showed toxicity on promastigotes but less toxicity against RAW 264.7 cell lines at different concentration (Table 3). This selectivity assay showed that the action of the compounds is specific for the protozoans and is not toxic for mammalian cells.

On the basis of their biological activities these compounds show potent leishmanicidal activity which may provide promising lead against leishmaniasis.

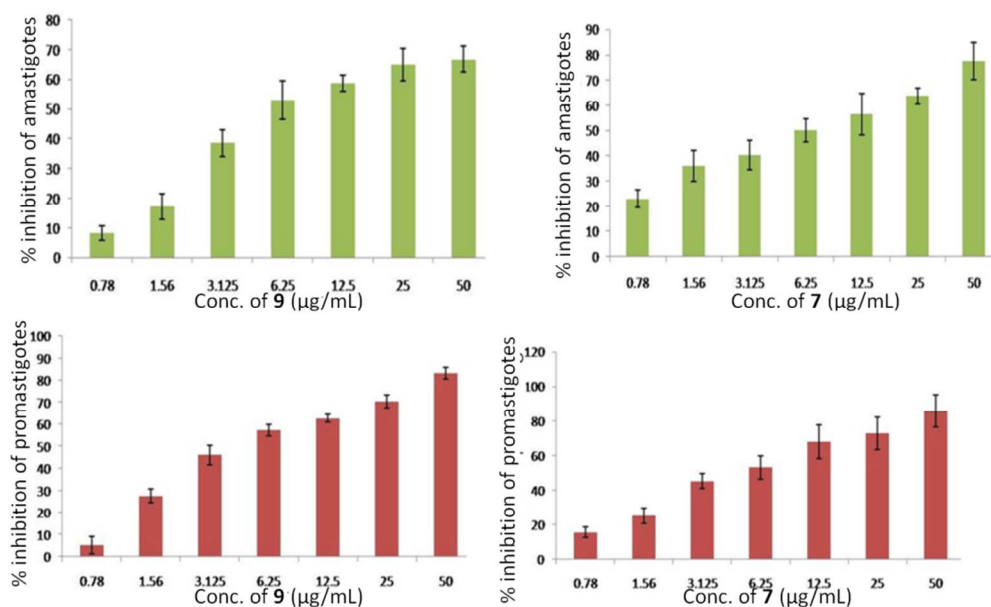


Fig.5 (a) Percentage inhibition in intracellular amastigote at different drug (complex 9) concentrations range (0.78 $\mu\text{g/mL}$ -50 $\mu\text{g/mL}$). (b) Percentage inhibition in intracellular amastigote at different drug (complex 7) concentration range (0.78 $\mu\text{g/mL}$ -50 $\mu\text{g/mL}$). (c) Percentage inhibition in promastigote at different drug (complex 9) concentration range (0.78 $\mu\text{g/mL}$ -50 $\mu\text{g/mL}$). (d) Percentage inhibition in promastigote on different drug (complex 7) concentration range (0.78 $\mu\text{g/mL}$ -50 $\mu\text{g/mL}$).

Table 3 Antileishmanial activity of compounds.

Compound	mw	IC ₅₀ (μg/mL) ±SD on promastigote forms of <i>L. donovani</i>	IC ₅₀ (μg/mL) ±SD on <i>L. donovani</i> intra-macrophage amastigotes forms	CC ₅₀ (μg/mL) ±SD on RAW 264.7 macrophage (μg/mL)	SI (CC ₅₀ /IC ₅₀ of intramacrophage amastigotes forms)
C ₂₀ H ₁₆ Pt BrO ₂ S ₄ 9	771.47	0.59±0.100	0.85±0.272	41.58±5.10	48.91
C ₂₈ H ₂₂ PdO ₂ S ₄ 7	625.14	0.56±0.10	1.99±0.08	31.68±11.80	15.91
Miltefosine		-	10.23±5.04	58.41±0.38	5.70

SI= Selectivity Index (SI defined by the ratio of CC₅₀ in RAW cells/IC₅₀ in intracellular *Leishmania* amastigotes).

Conclusions

Out of twelve **1-12** new fully characterized planar cis-chelated β-oxodithioester ligand complexes of Ni(II), Pd(II) and Pt(II), **7** and **9** formed with distinctly soft Pd(II) and Pt(II) and the ligands L3 and L1 having naphthyl and Br substituents showed efficient anti-leishmanial activity against both forms of *L. donovani* parasite that causes visceral leishmaniasis. These compounds were also found less cytotoxic at different concentrations on RAW264.7 cells. The crystal structures of **2-4**, **8** and **11** revealed distorted square planar geometry about the metal centres. The Pd and Pt complexes showed luminescent characteristic in CH₂Cl₂ solution originating from metal perturbed ILCT state. This study demonstrates the scope of the metal complexes with a wider range of functionalized β-oxodithioester ligands for their possible applications as anti-leishmanial agents.

Acknowledgements

NS, MKY (SRF) and GR (CSIR-SRF) gratefully acknowledge the financial support from the Council of Scientific and Industrial Research (CSIR), New Delhi, through project no. 01 (2679)/12/EMR-II, and the Department of Chemistry, CAS-UGC-I, Banaras Hindu University for the X-ray diffractometer.

Notes and references

^aDepartment of Chemistry, Faculty of Science, Banaras Hindu University,

Varanasi 221005, India. Fax: +91-542-2386127

E-mail: nsingh@bhu.ac.in, nsinghbhu@gmail.com

^bDepartment of Biochemistry, Faculty of Science, Banaras Hindu University, Varanasi-221005, India.

^cDepartment of Zoology, Faculty of Science, Banaras Hindu University, Varanasi- 221005, India.

^dDepartment of Chemistry, University of Reading, Whiteknights, Reading, RG6 6AD (U.K.)

[†]Electronic Supplementary Information (ESI) available: [¹H NMR for ligand and weak interactions table]. See DOI: 10.1039/b0000000x/

References

- (a) B. Rosenberg, *Naturwissenschaften*, 1973, **60**, 399-406; (b) B. Lippert, *Cisplatin: Chemistry and Biochemistry of a Leading Anticancer Drug*, B. Lippert, Ed. Wiley-VCH Verlag GmbH Weinheim, Germany, 1999; (c) C. X. Zhang and S. J. Lippard, *Curr. Opin. Chem. Biol.*, 2003, **7**, 481-489; (d) X. Y. Wang, *Anti-Cancer Agents Med. Chem.*, 2010, **10**, 396-411; (e) N. P. Farrell, *Curr. Top. Med. Chem.*, 2011, **11**, 2623-2631; (f) J. J. Wilson and S. J. Lippard, *Chem. Rev.*, 2014, **114**, 4470-4495; (g) X. Y. Wang and Z. J. Guo, *New Trends and Future Developments of Platinum-Based Antitumor Drugs*, in *Bioinorganic Medicinal Chemistry*, ed. E. Alessio, Wiley-VCH Verlag GmbH & Co. KGaA, Weinheim, 2011, 97-149.
- (a) V. K. Bhardwaj and A. Singh, *Inorg. Chem.*, 2014, **53**, 10731-10742; (b) E. B. Budzisz, M. Malecka, Ingo-Peter Lorenz, P. Mayer, R. A. Kwiecien, P. Paneth, U. Krajewska, and M. R. Zalski, *Inorg. Chem.*, 2006, **24**, 45.
- (a) A. Cavalli, and M. L. Bolognesi, *J. Med. Chem.*, 2009, **52**, 7339-7359; (b) J. Madureira, C. I. V. Ramos, M. Marques, C. Maia, B. de Sousa, L. Campino, M. G. Santana-Marques, and N. Farrell, *Inorg. Chem.*, 2013, **52**, 8881-8894; (c) H. Hussain, A. Al-Harrasi, A. Al-Rawahi, I. R. Green, and S. Gibbons, *Chem. Rev.*, 2014, **114**, 10369-10428; (d) A. S. Nagle, S. Khare, A. B. Kumar, F. Supek, A. Buchynskyy, C. J. N. Mathison, N. K. Chennamaneni, N. Pendem, F. S. Buckner, M. I. H. Gelb and V. Molteni, *Chem. Rev.*, 2014, **114**, 11305-11347.
- J. Alvar, S. Yactayo, and C. Bern, *Leishmaniasis and poverty. Trend in Parasitology*. 2006, **22**, 552-557.
- (a) S. Sundar and J. Chakravarty, *Expert Opin. Pharmacother*, 2013, **14**, 53-63; (b) A. Kulshrestha, R. Singh, D. Kumar, N. Singh Negi and P. Salotra, *Antimicrob Agents Chemother*, 2011, **55**, 2916-2961; (c) WHO (2007) *Leishmaniasis, background information*. <http://www.who.int/leishmaniasis/en/>. Retrieved on 2007-07-04.; (d) N. Singh., M. Kumar, R. K. Singh, *Asian Pacific Journal of Tropical Medicine*, 2012, 485-497.
- (a) A. S. Nagle, S. Khare, A. B. Kumar, F. Supek, A. Buchynskyy, C. J. N. Mathison, N. K. Chennamaneni, N. Pendem, F. S. Buckner, M. I. H. Gelb and V. Molteni, *Chem. Rev.*, 2014, **114**, 11305-11347; (b) H. Hussain, A. Al-Harrasi, A. Al-Rawahi, I. R. Green, and S. Gibbons, *Chem. Rev.*, 2014, **114**, 10369-10428.
- (a) M. I. Ali, M. K. Rauf, A. Badshah, I. Kumar, C. M. Forsyth, P. C. Junk, L. Kedzierski, and P. C. Andrews, *Dalton Trans.*, 2013, **42**, 16733-16741; (b) S. L. Croft, S. Sundar, and A. H. Fairlamb, *Clinical Microbiology Reviews*, 2006, **19**, 111-126.

- 8 P. C. Andrews, V. L. Blair, R. L. Ferrero, P. C. Junk, L. Kedzierskid, and R. M. Peirisa, *Dalton Trans.*, 2014, **43**, 1279-1291.
- 9 Y. C. Ong, V. L. Blair, L. Kedzierskib, and P. C. Andrews, *Dalton Trans.*, 2014, **43**, 12904-12916.
- 10 A. Martínez, T. Carreon, E. Iniguez, A. Anzellotti, A. Sánchez, M. Tyan, A. Sattler, L. Herrera, R. A. Maldonado and R. A. Sánchez-Delgado, *J. Med. Chem.*, 2012, **55**, 3867–3877.
- 11 (a) L. Otero, M. Vieites, L. Boiani, A. Denicola, C. Rigol, L. Opazo, C. Olea-Azar, J. D. Maya, A. Morello, R. L. Krauth-Siegel, O. E. Piro, E. Castellano, M. González, D. Gambino and H. Cerecetto, *J. Med. Chem.*, 2006, **49**, 3322–3331; (b) M. Vieites, L. Otero, D. Santos, C. Olea-Azar, E. Norambuena, G. Aguirre, H. Cerecetto, M. González, U. Kemmerling, A. Morello, J. Diego Maya and D. J. Gambino, *Inorg. Biochem.* 2009, **103**, 411–418; (c) M. Vieites, L. Otero, D. Santos, J. Toloza, R. Figueroa, E. Norambuena, C. Olea-Azar, G. Aguirre, H. Cerecetto, M. González, A. Morello, J. D. Maya, B. Garat and D. Gambino, *J. Inorg. Biochem.* 2008, **102**, 1033–1043; (d) B. Demoro, C. Sarniguet, R. Sánchez-Delgado, M. Rossi, D. Liebowitz, F. Caruso, C. Olea-Azar, V. Moreno, A. Medeiros, M. A. Comini, L. Otero and D. Gambino, *Dalton Trans.*, 2012, **41**, 1534–1543; (e) A. Merlino, L. Otero, D. Gambino and C. E. Laura, *Eur. J. Med. Chem.*, 2011, **46**, 2639–2651; (e) C. L. Donnici, M. H. Araujo, H. S. Oliveira, D. R. M. Moreira, V. R. A. Pereira, M. d. A. Souza, d. C. M. C. A. Brelaz and A. C. L. Leite, *Bioorg. Med. Chem.*, 2009, **17**, 5038–5043.
- 12 (a) M. Vieites, P. Smircich, B. Parajon-Costa, J. Rodriguez, V. Galaz, C. Olea-Azar, L. Otero, G. Aguirre, H. Cerecetto, M. Gonzalez, A. Gomez-Barrio, B. Garat and D. Gambino, *J. Biol. Inorg. Chem.*, 2008, **13**, 723–735; (b) P. I. d. S. Maia, A. G. d. A. Fernandes, J. J. N. Silva, A. D. Andricopulo, S. S. Lemos, E. S. Lang, U. Abram and V. M. Deflon, *J. Inorg. Biochem.*, 2010, **104**, 1276–1282.
13. (a) V. Meyer. *Ber.*, 1888, **21**, 353; (b) C. Alvarez-Toledano, J. Enriquez, R. A. Toscano, M. Martinez-Garcia, E. Cortes-Cortes, Y. M. Osornio, O. Garcia-Mellado and R. J. Gutierrez- Perez, *Organomet. Chem.*, 1999, **38**, 577; (c) C. Alvarez-Toledano, E. Delgado, B. Donnadiou, E. Hernandez, G. Martin and F. Zamora, *Inorg. Chim. Acta*, 2003, **351**, 119-122; (d) R. Saumweber, C. Robl and W. Weigand, *Inorg. Chim. Acta*, 1998, **269**, 83-90; (e) C. Mügge, R. Liu, H. Görls, C. Gabbiani, E. Michelucci, N. Rüdiger, J. H. Clement, L. Messori and W. Weigand, *Dalton Trans.*, 2014, **43**, 3072-3086.
14. G. Rajput, M. K. Yadav, M. G. B. Drew and N. Singh, *Dalton Trans.*, 2015, **44**, 5909-5916; (b) F. C. V. Larsson, S. O. Lawesson, *Tetrahedron*, 1972, **28**, 5341-5347; (c) R. Gompper, S. Schaefer, *Chem. Ber.*, 1967, **100**, 591-595; (d) K. Schubert, H. Görls, W. Weigand, *Z. Naturforsch.*, 2007, **62b**, 475.
15. Oxford Diffraction, CrysAlis CCD, RED, version 1.711.13, copyright (1995–2003), Oxford Diffraction Poland Sp.
16. G. M. Sheldrick, SHELXS97, Program for Crystal Structure Solution, University of Gottingen, Gottingen, 1997.
17. G. M. Sheldrick, SHELXL97, Program for Crystal Structure Refinement, University of Gottingen, Gottingen, 1997.
18. M. N. Burnett and C. K. Johnson, ORTEP-III, Oak Ridge Thermal Ellipsoid Plot Program for Crystal Structure Illustrations, Report ORNL-6895, Oak Ridge National Laboratory, Oak Ridge, TN, USA, 1996.
19. Mercury CSD 2.0 – New Features for the Visualization and Investigation of Crystal Structures; C. F. Macrae, I. J. Bruno, J. A. Chisholm, P. R. Edgington, P. McCabe, E. Pidcock, L. Rodriguez-Monge, R. Taylor, J. Van de Streek and P. A. Wood, *J. Appl. Crystallogr.*, 2008, **41**, 466–470,
20. (a) J. D. Berman, and D. J. Wyler, *J. Infect. Dis.*, 1980, **142**, 83-86; (b) J. D. Berman, *Journal of Parasitology*, 1984, **70**, 561-562; (c) J. D. Berman, and L. S. Lee, *Journal of Parasitology*. 1984, **70**, 220-225; (d) D. L. Looker, S. Martinez, J. M. Horton and J. J. Marr, *Journal of Infect. Dis.*, 1986, **154**, 323-327; (e) R. A. Neal, and S. L. Croft, *Journal of Antimicrobial Chemotherapy*, 1984, **14**, 463-475; (f) D. Sereno, and J. L. Lemesre, *Antimicrobial Agents and Chemotherapy*, 1997, **41**, 972-976.
- 21 K. Seifert, and S. L. Croft. *Antimicrob Agents Chemotherapy*, 2006, **50**, 73-79.
- 22 U. Sharma, D. Singh, P. Kumar, M. P. Dobhal and S. Singh, *Indian J. Med. Res.*, 2011, **134**, 709-716.
- 23 (a) I. Garcia-Orozco, J. G. Lopez-Cortes M. Carmen Ortega-Alfaro, R. A. Toscano, G. Penieres-Carrillo, and C. Alvarez-Toledano, *Inorg. Chem.*, 2004, **43**, 8572-8576; (b) I. Garcia-Orozco, Ma. Carmen Ortega-Alfaro, J. G. Lopez-Cortes, R. A. Toscano, and C. Alvarez-Toledano, *Inorg. Chem.*, 2006, **45**, 1766-1773.
- 24 (a) R. Saumweber, C. Robl and W. Weigand, *Inorg. Chim. Acta*, 1998, **269**, 83-90.
- 25 N. Singh, B. Singh, K. Thapliyal and M. G. B. Drew, *Inorg. Chim. Acta*, 2010, **363**, 3589–3596.